

RESEARCH ARTICLE | APRIL 04 2024

Stabilization of hydrogen-bonded molecular chains by carbon nanotubes

Special Collection: [Topics in Nonlinear Science: Dedicated to David K. Campbell's 80th Birthday](#)

Alexander V. Savin ; Yuri S. Kivshar  

 Check for updates

Chaos 34, 043111 (2024)

<https://doi.org/10.1063/5.0197401>



View
Online



Export
Citation



Chaos

Special Topic: Nonautonomous Dynamics
in the Climate Sciences

Submit Today

Stabilization of hydrogen-bonded molecular chains by carbon nanotubes

Cite as: Chaos 34, 043111 (2024); doi: 10.1063/5.0197401

Submitted: 13 January 2024 · Accepted: 14 March 2024 ·

Published Online: 4 April 2024



View Online



Export Citation



CrossMark

Alexander V. Savin^{1,2,a)}  and Yuri S. Kivshar^{3,b)} 

AFFILIATIONS

¹Semenov Institute of Chemical Physics, Russian Academy of Sciences, Moscow 119991, Russia

²Academic Department of Innovational Materials and Technologies Chemistry, Plekhanov Russian University of Economics, Moscow 117997, Russia

³Nonlinear Physics Center, Research School of Physics, Australian National University, Canberra, ACT 2601, Australia

Note: This paper is part of the Focus Issue on Topics in Nonlinear Science: Dedicated to David K. Campbell's 80th Birthday.

^{a)}asavin@chph.ras.ru

^{b)}Author to whom correspondence should be addressed: yuri.kivshar@anu.edu.au

ABSTRACT

We study numerically nonlinear dynamics of several types of molecular systems composed of hydrogen-bonded chains placed inside carbon nanotubes with open edges. We demonstrate that carbon nanotubes provide a stabilization mechanism for quasi-one-dimensional molecular chains via the formation of their secondary structures. In particular, a polypeptide chain $(\text{Gly})_N$ placed inside a carbon nanotube can form a stable helical chain (3_{10} -, α -, π -, and β -helix) with parallel chains of hydrogen-bonded peptide groups. A chain of hydrogen fluoride molecules $\cdots \text{FH} \cdots \text{FH} \cdots \text{FH}$ can form a hydrogen-bonded zigzag chain. Remarkably, we demonstrate that for molecular complexes $(\text{Gly})_N \in \text{CNT}$ and $(\text{FH})_N \in \text{CNT}$, the hydrogen-bonded chains will remain stable even at $T = 500$ K. Thus, our results suggest that the use of carbon nanotubes with encapsulated hydrogen fluoride molecules may be important for the realization of high proton conductivity at high temperatures.

Published under an exclusive license by AIP Publishing. <https://doi.org/10.1063/5.0197401>

The dynamics of quasi-one-dimensional molecular systems with hydrogen-bonded chains (helix of protein, chain of hydrogen fluoride molecules) located inside open carbon nanotube is numerically modeled. It is shown that a polypeptide chain placed inside a carbon nanotube, depending on its diameter, takes the form of a stable helical chain (3_{10} -, α -, π -, and β -helix) with parallel arrays of hydrogen-bonded peptide groups. Hydrogen fluoride molecules placed inside nanotubes of small radii create hydrogen-bonded zigzag chains along which proton transport can occur. In such molecular systems, the hydrogen-bonded chains retain their structure and the interaction with the nanotubes lead to their additional stabilization. For some molecular complexes, the hydrogen-bonded chains will remain stable even at $T = 500$ K.

I. INTRODUCTION

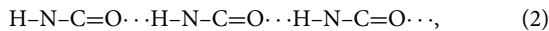
One of the research activities of David Campbell has been devoted to the study of nonlinear waves and solitons in discrete systems,^{1,2} including the pioneering results on nonlinear dynamics

of polyacetylene $[(\text{CH})_x]$.³ Many of the discrete nonlinear models are inspired by the physics of molecular systems. Realistic molecular systems have a complex multi-component structure, consisting of nonlinearly interacting subsystems (electronic, excitonic, phononic, ionic, proton). In such systems, stable propagation of nonlinear waves (such as polarons, solitons, kinks,) can be observed when nonlinear effects compensate for linear dispersion. As a special example, highly efficient energy and charge transfer takes place in molecular chains with hydrogen bonds.

Molecular systems with hydrogen bonds are characterized by a relatively low stabilization energy (0.12–0.40 eV per hydrogen bond), which ensures their high dynamic mobility. Such structures include α -helices and β -sheets of proteins,^{4,5} DNA double helices, organic crystals of acetamides [e.g., acetanilide $(\text{CH}_3\text{CONHC}_6\text{H}_5)_x$],^{6,7} crystals of aramides (Kevlar crystals⁸), proton transport channels in cell membranes,^{9–12} crystals of alcohols, hydrogen halides,^{13,14} and some other systems.

However, many of the molecular systems studied theoretically are restricted by the assumption of low dimensionality, so they become unstable being placed into three-dimensional space.

chains of hydrogen-bonded HNCO peptide groups (PGs),



where the lines represent the valence bonds and the dots the represent hydrogen bonds. According to Davydov's theory, these chains can transport energy released during the hydrolysis of the adenosine triphosphate (ATP) molecule in the form of self-localized states of vibrations of amide-I double valence bonds C=O, which are part of PG. The self-localization of the amid-I vibration is caused by its non-linear interaction with longitudinal deformations of the hydrogen bond chains (2). Using this model, it was shown that in α -helical protein molecules, nonlinear collective self-localized excitations can propagate without energy loss and shape change, which were later called *Davydov solitons*.^{34–38}

In the first papers by Davydov *et al.*, the continuum approximation was used and the α -helix was treated as a continuous medium. The discrete model was used to numerically model the dynamics of Davydov solitons in the work of Scott *et al.*^{34,35} These works have led to an increased interest in the Davydov model.^{39–45} The Davydov model is still actively used today (see Refs. 46–50).

The presence of hydrogen bonding chains (2) also allows for the possibility of external electron transfer in α -helical proteins in the form of an electrosoliton (a bound state of a localized electron with the region of helix deformation resulting from the interaction of the electron with the PG chains).^{51–53}

Practically, all molecular complexes with hydrogen bonding chains are no longer stable at high temperatures (at $T > 100^\circ\text{C}$ all hydrogen bonding chains are destroyed). This complicates the use of such molecular systems in nanotechnology. In this work, it will be shown that the use of complexes of such molecular systems with carbon nanotubes can significantly increase the stability of the hydrogen bond chains. For this purpose, quasi one-dimensional molecular systems (α -helix of protein, zigzag chain of hydrogen fluoride molecules) will be placed in carbon nanotubes of a certain radius. In this case, the hydrogen bonding chains will retain their structure and the interaction with the nanotube will lead to their additional stabilization, which will allow them to be used for energy and charge transfer over a wider temperature range. In such composite systems, the hydrogen bonding chains will remain stable even at $T = 500\text{ K}$.

III. HELICES OF PROTEIN MOLECULES

In order to analyze the helical structures, we consider a polypeptide chain $(\text{Gly})_N$ composed of N peptide groups, described by the chemical formula,



where three hydrogen atoms are attached to the first α -carbon atom and one hydrogen atom is attached to the nitrogen atom of the last peptide group.

For numerical modeling, a polyglycine chain (3), we consider α -carbon atoms with attached hydrogen atoms as one hybrid atom C_α . In this case, each chain consists of five atoms C_α , C, O, N, and H with the coordinates $\{\mathbf{u}_{n,i}\}_{i=1}^5$, where n is the link number of the polypeptide chain, and i is the atomic number. The atomic masses are $M_{n,1} = 14m_p$, $M_{n,2} = 12m_p$, $M_{n,3} = 16m_p$, $M_{n,4} = 14m_p$,

$M_{n,5} = m_p$ (for the end links $M_{1,1} = 15m_p$, $M_{N,4} = 15m_p$), where $m_p = 1.6603 \times 10^{-27}\text{ kg}$ —the mass of a proton. To study numerically the interatomic interaction, we employ the AMBER general force field for organic molecules (version 2.1, April 2016).⁵⁴

We write the Hamiltonian of a polypeptide chain in the form,

$$H = \sum_{n=1}^N \sum_{i=1}^5 \left[\frac{1}{2} (M_{n,i} \dot{\mathbf{u}}_{n,i} \cdot \dot{\mathbf{u}}_{n,i}) + P(\{\mathbf{u}_{n,i}\}_{n=1,i=1}^{N,5}) \right]. \quad (4)$$

Here, the first sum defines the kinetic energy, with the three-dimensional vector $\mathbf{u}_{n,i} = (x_{n,i}, y_{n,i}, z_{n,i})$ defining the coordinates of the i th atom of the n th chain link. The second sum describes the potential energy of the chain determined with the AMBER force field approach.

For the stationary state of the chain, we need to solve numerically the problem of the minimum potential energy,

$$P \rightarrow \min : \{\mathbf{u}_{n,i}\}_{n=1,i=1}^{N,5}. \quad (5)$$

The solution of problem (5) depends on the choice of the initial configuration of the chain. The configurations obtained from modeling the dynamics of a polypeptide chain in a carbon nanotube were used to solve the problem. Due to spatial constraints, such configurations always have the form of a chain directed along the nanotube. By changing the radius of the nanotube we can obtain all possible helical configurations. The numerical solution of problem (5) showed that polypeptide chain (3) has four stationary states as a helix chain: 3_{10} -helix, α -helix, π -helix, and β -helix—see Fig. 2. We assume that the peptide groups n and k ($n < k$) form a hydrogen bond with the nonvalent interaction energy of the corresponding chain links defined as

$$E_{n,k} = U(\{\mathbf{u}_{n,i}\}_{i=1}^5, \{\mathbf{u}_{k,j}\}_{j=1}^5) < -0.16\text{ eV}.$$

We noticed that the distance between N and O atoms determined by the presence of a hydrogen bonding between the peptide groups is not a good measure, since the bonding energy depends not only on the distance of these atoms but also on the mutual orientation of the peptide groups.

Each helix is characterized by the steady state energy E , the number of hydrogen bond chains N_{sp} , the number of hydrogen bonds N_{hb} , the average bond energy

$$E_{\text{hb}} = - \sum_{l=1}^{N_{\text{hb}}} E_{n_l, k_l} / N_{\text{hb}}, \quad (6)$$

and the length of the helix (the distance between the end alpha carbon atoms $L = |\mathbf{u}_{N,1} - \mathbf{u}_{1,1}|$).

The chain of $N = 73$ peptide groups was used to analyze the helical structures. The values of E , N_{sp} , N_{hb} , E_{hb} , and L for different stationary states (conformations) of the polypeptide chain $(\text{Cly})_{73}$ are given in Table I. As can be seen from the table, the most energetically unfavorable structure is the 3_{10} -helix. Such a helix is highly stretched, it has two chains of weakened hydrogen bonds—see Fig. 2. Further more favorable in energy are the α -, π -, β -helix and globule structures.

We study the dynamics of helical structures by placing the polypeptide chain in a Langevin thermostat at temperature T and

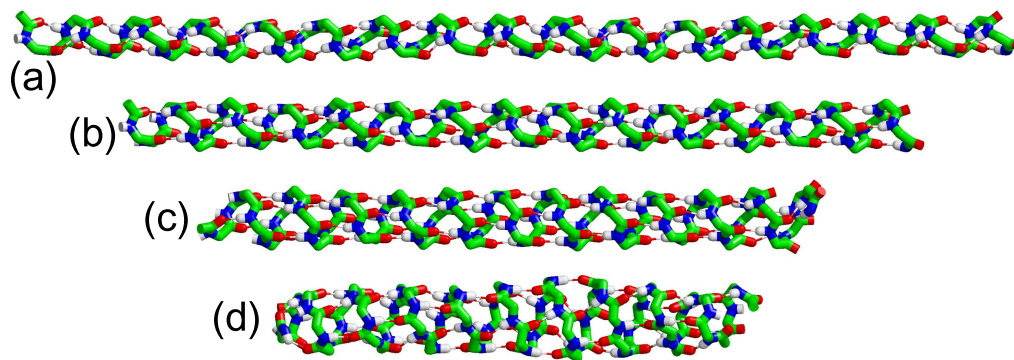


FIG. 2. Helical structures of the peptide chain (Gly)₅₂: (a) 3₁₀-helix (stationary structure energy $E = 16.26$ eV, hydrogen bond energy $E_{\text{hb}} = 0.175$ eV, length $L = 9.66$ nm); (b) α -helix ($E = 12.00$, $E_{\text{hb}} = 0.258$, $L = 7.64$); (c) π -helix ($E = 11.32$, $E_{\text{hb}} = 0.268$, $L = 6.01$); (d) β -helix ($E = 10.03$, $E_{\text{hb}} = 0.268$, $L = 4.67$). Carbon atoms are shown in green, nitrogen atoms in blue, oxygen atoms in red, and hydrogen atoms in white. Hydrogen bonds are shown as thin lines. Hydrogen atoms of α -carbon atoms are not shown.

study numerically the dynamics of the system for the time period of $t = 100$ ns. To do this, we integrate numerically the system of Langevin equations,

$$M_{n,i} \ddot{\mathbf{u}}_{n,i} = - \frac{\partial H}{\partial \mathbf{u}_{n,i}} - \Gamma M_{n,i} \dot{\mathbf{u}}_{n,i} - \Xi_{n,i}, \quad n = 1, \dots, N, \quad i = 1, \dots, 5, \quad (7)$$

where $\Gamma = 1/t_r$ is the friction coefficient and $\Xi_{n,i} = \{\xi_{n,i,k}\}_{k=1}^3$ is the three-dimensional vector of normally distributed random Langevin forces with the following correlations:

$$\langle \xi_{n_1,i,k}(t_1) \xi_{n_2,j,l}(t_2) \rangle = 2M_{n_1,i} k_B T \Gamma \delta_{n_1,n_2} \delta_{ij} \delta_{kl} \delta(t_1 - t_2).$$

Here, $M_{n,i}$ is the mass of the i th atom of the n th segment of polypeptide chain, k_B is the Boltzmann constant, and T is temperature of the Langevin thermostat, numbers $n_1, n_2 = 1, \dots, N$, $i, j = 1, \dots, 5$, $k, l = 1, 2, 3$. The parameter $t_r = 10$ ps characterizes the intensity of energy exchange between the molecular system and the thermostat.

The equations of motion Eq. (7) are solved numerically using the velocity Verlet method.⁵⁵ A time step of 1 fs is used in the simulations, since further reduction in the time step has no appreciable effect on the results.

Let us numerically integrate the system of equations of motion (7) with the initial condition corresponding to the stationary state of the polypeptide chain. After the dynamics of the molecular system

TABLE I. Energy E , number of hydrogen bond chains N_{sp} , number of hydrogen bonds N_{hb} , average hydrogen bond energy E_{hb} , and chain end distance L for different stationary states (conformations) of the polypeptide chain (Gly)₇₃.

Conformation	E (eV)	N_{sp}	N_{hb}	E_{hb} (eV)	L (nm)
3 ₁₀ -helix	22.56	2	71	0.1704	13.59
α -helix	16.22	3	70	0.2583	10.79
π -helix	14.93	4	69	0.2695	8.46
β -helix	14.00	5	70	0.2560	5.94
globule	13.33	...	60	0.2341	0.57

reaches the steady state, we will find the time averages of the system energy $\bar{E}(T)$, the number of hydrogen bonds $\bar{N}_{\text{hb}}(T)$, and chain length $\bar{L}(T)$.

The state of the system can be conveniently characterized by its dimensionless heat capacity,

$$c = \frac{1}{15Nk_B} \frac{d\bar{E}(T)}{dT}, \quad (8)$$

the normalized number of hydrogen bonds $n_{\text{hb}} = \bar{N}_{\text{hb}}(T)/N$ and chain length $\bar{L}(T)$. The dependence of these quantities on temperature is shown in Fig. 3.

The 3₁₀-helix is the most unstable. At temperature $T = 10$ K, it changes to π -helix. The alpha-helix of the chain remains stable at $T < T_1 = 95$ K; at $T_1 < T < T_2 = 235$ K, the α -helix changes into π -helix; and at $T_2 < T < T_3 = 285$ K, that changes into β -helix. At $T \geq T_3$, the chain transforms into a globule shape—see Fig. 3. The π -helix remains stable at $T < T_2$, and at $T = T_2$, it changes into a β -helix. The beta helix is stable at $T < T_3$, and at $T > T_3$, the chain adopts the globule form. The transitions between the forms of the helix occur without changing the heat capacity of the molecular system; i.e., these are second-order phase transitions. The increase in the heat capacity occurs only when the chain transitions to the globular form. The temperature $T = T_3$ can be considered the melting point of the β -helix. The transition of a helix into a globule is first-order phase transition; here, the dimensionless heat capacity increases from $c = 1$ to $c = 1.2$.

Thus, in an isolated polyglycine peptide chain, regular chains of hydrogen bonds (2) can only exist at low temperatures $T < 285$ K.

IV. CONFORMATIONS OF A PEPTIDE CHAIN INSIDE A CARBON NANOTUBE

Polypeptide molecules tend to self-insertion into carbon nanotubes with open ends. Inside the nanotube, polypeptide atoms are able to fully realize non-valent interactions with its surface.^{56–58} This is particularly significant for hydrophobic polypeptides such as (Gly)_N, (Ala)_N, (Val)_N, (Ile)_N. Let us determine what conformations

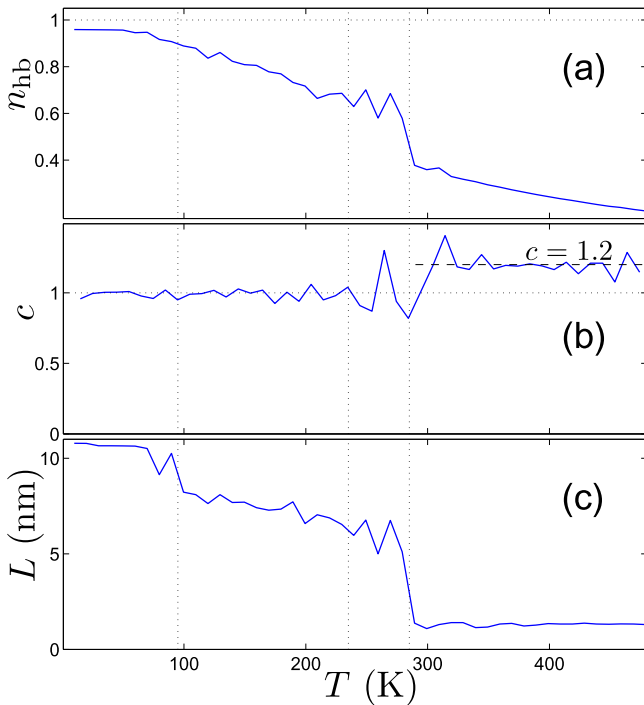


FIG. 3. Dependence of (a) the normalized number of hydrogen bonds η_{hb} , (b) the dimensionless heat capacity c , and (c) the chain end spacing \bar{L} for a polypeptide chain (Gly)₇₃ originally shaped as a α -helix. The vertical lines indicate the temperature values of 95, 235, and 285 K.

the polypeptide chain (Gly) _{N} inside a single-walled carbon nanotube with chirality index (n, m) (CNT _{(n,m)}) can take.

To describe the dynamics of the CNT, we present the nanotube Hamiltonian in the form,

$$H_c = \sum_{n=1}^{N_c} \left[\frac{1}{2} M_{n,0} (\dot{\mathbf{v}}_n, \dot{\mathbf{v}}_n) + Q_n \right], \quad (9)$$

where N_c is the number of atoms in the CNT, and $M_{n,0}$ is the mass of n th carbon atom, $\mathbf{v}_n = \{\mathbf{v}_{n,i}(t)\}_{i=1}^3$ is the radius vector of n th atom at the time t . The term Q_n describes the interaction energy of the atom with index n with neighboring atoms.

To describe the carbon-carbon valence interactions, let us use a standard set molecular dynamics potentials.^{59,60} We consider a hydrogen-terminated nanotube with open ends, where the edge atoms correspond to the molecular group CH. We will consider such a group as a single effective particle at the location of the carbon atom. Therefore, in our model of open CNT, we take the mass of atoms inside the nanotube as $M_{n,0} = 12m_p$ and for the edge atoms as $M_{n,0} = 13m_p$.

The valence bond between two neighboring carbon atoms n and k can be described by the Morse potential,

$$U_1(\mathbf{v}_n, \mathbf{v}_k) = \varepsilon_1 \left\{ \exp[-\alpha(r_{nk} - r_1)] - 1 \right\}^2, \quad (10)$$

where $r_{nk} = |\mathbf{v}_n - \mathbf{v}_k|$, $\varepsilon_1 = 4.9632$ eV is the valence bond energy, and $r_1 = 1.418$ Å is the equilibrium valence bond length.

The valence angle deformation energy between three adjacent carbon atoms n, k , and l can be described by the potential,

$$U_2(\mathbf{v}_n, \mathbf{v}_k, \mathbf{v}_l) = \varepsilon_2 (\cos \varphi - \cos \varphi_0)^2, \quad (11)$$

where $\cos \varphi = (\mathbf{v}_n - \mathbf{v}_k, \mathbf{v}_l - \mathbf{v}_k) / r_{nk} r_{kl}$, and $\varphi_0 = 2\pi/3$ is the equilibrium valent angle. Parameters $\alpha = 1.7889$ Å⁻¹ and $\varepsilon_2 = 1.3143$ eV can be found from the small-amplitude oscillation spectrum of the graphene sheet.⁶¹ Valence bonds between four adjacent carbon atoms n, m, k , and l constitute torsion angles, whose potential energy can be defined as

$$U_3(\phi) = \varepsilon_3 (1 - \cos \phi), \quad (12)$$

where ϕ is the corresponding torsion angle ($\phi = 0$ is the equilibrium value of the angle) and $\varepsilon_3 = 0.499$ eV. A detailed discussion about the choice of the interatomic potential parameters can be found in Ref. 59.

We describe the interaction of polypeptide chain atoms with nanotube atoms using Lennard-Jones potentials with parameters from the AMBER force field.

The Hamiltonian of the molecular system (Gly) _{N} ∈ CNT will have the form,

$$H = \sum_{n=1}^{N_c} \frac{1}{2} (M_{n,0} \dot{\mathbf{v}}_n, \dot{\mathbf{v}}_n) + \sum_{n=1}^N \sum_{i=1}^5 \frac{1}{2} (M_{n,i} \dot{\mathbf{u}}_{n,i}, \dot{\mathbf{u}}_{n,i}) + E(\{\mathbf{v}_n\}_{n=1}^{N_c}, \{\mathbf{u}_{n,i}\}_{n=1, i=1}^{N,5}), \quad (13)$$

where the first summand defines the kinetic energy of the carbon nanotube (N_c is the number of atoms of the nanotube), the second defines the kinetic energy of the polypeptide chain, and the third defines the interaction energy of the atoms of the system.

To find the stationary state of the two-component system (Gly) _{N} ∈ CNT, it is necessary to solve numerically the problem on the minimum of the interaction energy,

$$E \rightarrow \min : \{\mathbf{v}_n\}_{n=1}^{N_c}, \{\mathbf{u}_{n,i}\}_{n=1, i=1}^{N,5}. \quad (14)$$

Let us take the polypeptide chain (Gly)₇₃ and place it inside a nanotube of length $L_{cnt} = 16.1$ nm. The numerical solution of problem (14) shows that the polypeptide chain inside the nanotube takes the form of a helix, the type of which depends on the radius of the nanotube R —see Table II. Thus, at $R < 5$ Å, the chain inside the nanotube can take only one stationary state—helix 3₁₀. Two stationary states of the chain helix 3₁₀- and α -helix are possible inside the nanotube (13,0)—see Figs. 4(a) and 4(b). The α -helix can exist in all nanotubes with radius $R > 5.1$ Å, and π -helix—in nanotubes with $R > 5.9$ Å, β -helix—in nanotubes with $R > 6.1$ Å. Note that in nanotubes with $R < 5$ Å, hydrogen bonds become strong for 3₁₀-helix, the strongest interaction between the polypeptide chain and the nanotube occurs here (the smaller the radius of the nanotube, the greater the interaction energy).

Let us consider the dynamics of the (Gly)₇₃ ∈ CNT complex. To do this, we place the nanotube in a Langevin thermostat of temperature T (the thermalization of the polypeptide chain inside the CNT will occur through its interaction with the nanotube) and numerically simulate the dynamics of the molecular complex during the

TABLE II. Values of the nanotube radius R , the helix type of the polypeptide chain, the energy E of the stationary state of the complex $(\text{Gly})_{73} \in \text{CNT}_{(n,m)}$, the interaction energy E_i of the polypeptide chain with the nanotube, and the average hydrogen bonding energy E_{hb} for different nanotubes with chirality index (n, m) (nanotube length $L_{\text{cnt}} = 16.1 \text{ nm}$). The positive value of the complex energy E is due to the fact that in a cylindrical nanotube, unlike a flat nanoribbon, the valence bonds are always not in the ground state. The smaller the radius of the nanotube, the more tense the valence bonds are and, therefore, the higher the value of the energy. The energy E_{hb} is positive due to its definition—see formula (6).

(n, m)	R (Å)	Helix	E (eV)	$-E_i$ (eV)	E_{hb} (eV)
(12,0)	4.74	3_{10}	221.53	39.16	0.2756
(7,7)	4.76	3_{10}	219.25	39.66	0.2744
(13,0)	5.13	3_{10}	204.16	37.33	0.2005
		α	203.88	33.39	0.2711
(8,8)	5.43	α	188.93	34.06	0.2618
(14,0)	5.52	α	186.57	33.65	0.2584
(15,0)	5.91	α	178.93	28.74	0.2314
		π	175.29	30.87	0.2705
(9,9)	6.11	α	175.68	25.53	0.2481
		π	170.79	29.12	0.2641
		β	171.71	30.33	0.2588
(16,0)	6.29	α	172.18	24.25	0.2558
		π	167.92	27.03	0.2614
		β	167.64	28.63	0.2532
(17,0)	6.68	α	164.70	21.74	0.2568
		π	161.99	22.92	0.2652
		β	157.05	27.68	0.2708
(10,10)	6.78	α	162.77	21.06	0.2555
		π	160.16	22.15	0.2658
		β	155.55	26.46	0.2700
(18,0)	7.07	α	157.64	19.89	0.2587
		π	155.23	20.83	0.2659
		β	152.06	23.31	0.2653
(11,11)	7.46	α	150.77	18.48	0.2570
		π	148.85	19.33	0.2660
		β	146.56	20.24	0.2636

time $t = 20 \text{ ns}$. To do this, we numerically integrate the system of Langevin equations,

$$M_{n,0} \ddot{\mathbf{v}}_n = -\frac{\partial H}{\partial \mathbf{v}_n} - \Gamma M_{n,0} \dot{\mathbf{v}}_n - \Theta_n, \quad n = 1, \dots, N_c, \quad (15)$$

$$M_{n,i} \ddot{\mathbf{u}}_{n,i} = -\frac{\partial H}{\partial \mathbf{u}_{n,i}}, \quad n = 1, \dots, N, \quad i = 1, \dots, 5, \quad (16)$$

where $\Theta_n = \{\eta_{n,k}\}_{k=1}^3$ is three-dimensional vector of normally distributed random Langevin forces with the following correlations:

$$\langle \eta_{n_1,k}(t_1) \eta_{n_2,l}(t_2) \rangle = 2M_{n_1,0} k_B T \delta_{n_1,n_2} \delta_{kl} \delta(t_1 - t_2).$$

We numerically integrate the system of equations of motion (15) and (16) with the initial condition corresponding to the solution of the minimum problem (14). After the dynamics of the molecular complex reaches the steady state, we will find the time averages of

the complex energy $\bar{E}(T)$, the number of hydrogen bonds $\bar{N}_{\text{hb}}(T)$, and peptide chain length $\bar{L}(T)$.

The state of the molecular complex can be characterized by its dimensionless heat capacity,

$$c = \frac{1}{3(N_c + 5N)k_B} \frac{d\bar{E}(T)}{dT}, \quad (17)$$

the normalized number of hydrogen bonds $n_{\text{hb}} = \bar{N}_{\text{hb}}(T)/N$ and peptide chain length $\bar{L}(T)$. The dependence of these quantities on temperature for different nanotubes is shown in Figs. 5 and 6.

Numerical integration of the system of equations of motion (15) and (16) showed that at $T < 500 \text{ K}$, there is only one basic helix type for each nanotube. For $\text{CNT}_{(13,0)}$, the 3_{10} -helix will be the basic helix. Here, at $T < 75 \text{ K}$, two forms of helix can exist: 3_{10} - and α -helix, and at $T > 75 \text{ K}$, only the 3_{10} -helix can exist (thermal fluctuations lead to the transition of the α -helix to the 3_{10} -helix)—see Figs. 4 and 5. The 3_{10} helix exists at all temperatures $T < 500 \text{ K}$. As the temperature increases, only partial breaking of the edge hydrogen bonds occurs, leading to a decrease in n_{hb} and an increase in the peptide chain length \bar{L} . The dimensionless heat capacity of the $(\text{Gly})_{73} \in \text{CNT}_{(13,0)}$ complex remains constant at $c = 1$.

Note that for an isolated peptide chain, the 3_{10} -helix form is the most unstable. Even at $T = 10 \text{ K}$, thermal fluctuations lead to a rapid transition to the π -helix, and at $T = 285 \text{ K}$, the chain melts (the chain changes from helical to molten globule form).

In nanotube (8,8), the ground state of the peptide chain will always be α -helix; in $\text{CNT}_{(9,9)}$, that will be π -helix; and in $\text{CNT}_{(10,10)}$, that will be β -helix. The appearance of these helical states of the peptide chain in nanotubes with chirality indices (8,8), (9,9), and (10,10) is shown in Fig. 7. All these helices are stable to thermal fluctuations at $T < 500 \text{ K}$. With increasing temperature, there is only a small decrease in the number of hydrogen bonds—see Fig. 6(a). At the same time, the dimensionless heat capacity always remains equal to one and the length of the helix is almost unchanged—see Figs. 6(b) and 6(c).

Thus, placing a polypeptide chain in a nanotube of small radius will stabilize its helical shape. For the simplest polypeptide chain $(\text{Gly})_N$, the most stable to thermal fluctuations will be the α -helix lying inside the nanotube (9,9). Here, the α -helix is conserved at all temperatures $T < 500 \text{ K}$. Note that such stabilization of the helical shape is impossible for an isolated polypeptide chain. Note that the optimal nanotube radius for helix stabilization depends on the size of the amino acid residues. For larger Ala, Val, Ile residues, the best stabilization will occur in nanotubes of larger radius.

V. HYDROGEN-BONDED CHAINS OF HYDROGEN FLUORIDE MOLECULES

As was shown in a number of theoretical and experimental studies of water-filled carbon nanotubes,^{62–66} water molecules can move inside open-edged nanotubes and form extended hydrogen bond chains. Small-diameter nanotubes with a chain of water molecules inside can act as proton-conducting channels.^{67,68}

Carbon nanotubes are hydrophobic, and the presence of water molecules inside them is not energetically favorable. Inside the nanotube, water molecules cannot organize a three-dimensional lattice of hydrogen bonds. For example, inside a $\text{CNT}_{(6,6)}$ (diameter

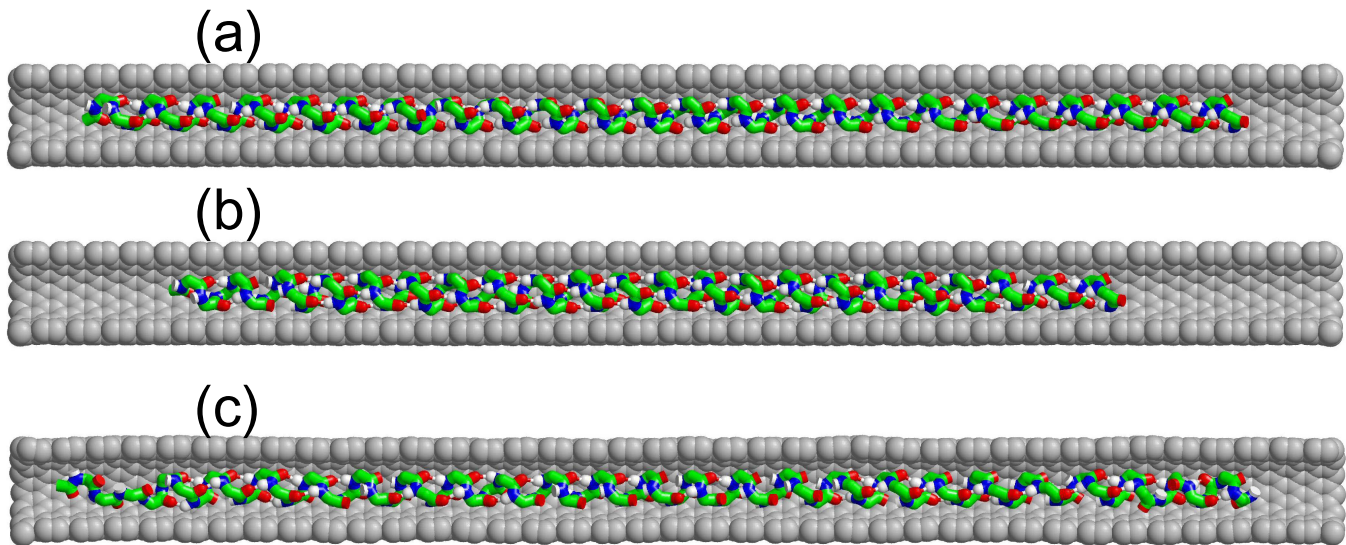
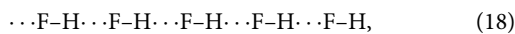


FIG. 4. State of the polypeptide chain $(\text{Gly})_{73}$ located in the nanotube (13,0) with open edges: (a) 3_{10} -helix ($T = 10$ K), (b) α -helix at $T = 10$ K, and (c) $T = 300$ K (the peptide chain is 3_{10} -helix). For ease of review, only one half of the nanotube atoms is shown (nanotube atoms are shown in gray). The length of the nanotube is $L_{\text{CNT}} = 16.14$ nm, and the number of carbon atoms is $N_c = 1976$.

$D = 0.80$ nm), only one chain of water molecules can be found, in which each molecule participates in the formation of two hydrogen bonds (in the bulk phase, each molecule participates in the formation of four bonds).⁶⁹

Hydrogen fluoride molecules FH can also form zigzag chains of hydrogen bonds $(\text{FH})_{\infty}$,



which are similar to zigzag chains of hydroxyl groups (1). At temperature $T < 189.6$ K, hydrogen fluoride has a crystal structure formed by parallel flat hydrogen bond chains.⁷⁰ Note that a separate zigzag chain of hydrogen bonds (18) becomes unstable in three-dimensional space. The chain breaks down into cyclic chains of small size, the most stable being chains of six molecules in the shape of a regular hexagon.⁷¹ Hydrogen bond chains (18) can be stabilized by placing them inside the CNT, i.e., forming a $(\text{FH})_{\infty} \in \text{CNT}$ structure.

One hydrogen fluoride molecule can participate in the formation of two hydrogen bonds in each chain (18). The study of interaction of the $\text{F}-\text{H} \cdots \text{F}-\text{H}$ dimer with CNT reveals that for the hydrogen fluoride dimer, it is energetically more favorable when the dimer is placed inside the nanotube.⁷² As a result, being placed inside open CNTs, $(\text{FH})_N$ chains can form stable $(\text{FH})_N \in \text{CNT}$ structures (N —number of hydrogen fluoride molecules). Keeping hydrogen fluoride inside nanotubes may help to avoid problems associated with its high toxicity.⁷³

We simulate numerically molecular complexes $(\text{FH})_N \in \text{CNT}$ by describing the valence bond deformation of the two-atom FH molecule with a harmonic potential,

$$V(\rho) = \frac{1}{2} K(\rho - \rho_0)^2, \quad (19)$$

where ρ and $\rho_0 = 0.929$ Å are the current and equilibrium bond lengths, respectively, and $K = 444.3$ N/m is the bond stiffness.

The interaction of FH molecules is conveniently described by the potential 12-6-1,^{71,74}

$$U = \sum_{i=1}^3 \sum_{j=1}^3 \kappa q_i q_j / r_{ij} + 4\epsilon [(\sigma/r)^{12} - (\sigma/r)^6], \quad (20)$$

where the first sum defines the Coulomb interaction between systems of point charges approximating the charge distribution in a pair of interacting FH molecules (r_{ij} describes the distance between the charge q_i of the first molecule and the charge q_j of the second molecule), r stands for the distance between the centers of the fluorine atoms, and the coefficient $\kappa = 14.400611$ eVÅ/e². Two positive charges q_2, q_3 are on atoms F and H, and the negative charge $q_1 = -(q_2 + q_3)$ is at a distance r_1 from atom F on the interval [FH]. If potential (20) does not fix the position of the two charges on the atoms of the molecule, the potential will be given by seven parameters: two charges, three distances $\{r_i\}_{i=1}^3$, specifying the position of the charges on the line connecting atoms F and H, and two parameters ϵ and σ of the Lenard-Jones potential.

We noticed that the sufficiently large number of free parameters of the 12-6-1 potential allows an efficient modeling of the dynamics of two-atom FH molecule complexes. Usually, the FH molecule participates in the formation of two strong hydrogen bonds. We assume that when the valence bond length $r = |\text{FH}|$ changes, the distances between the charges from the center of the fluorine atom also change proportionally. To model numerically the dynamics of hydrogen bond chains (18), we employ potential (20)

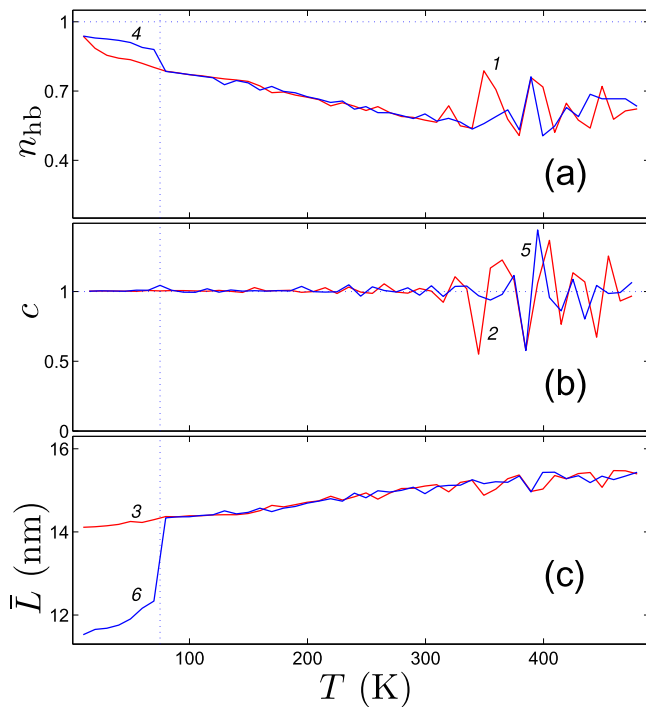


FIG. 5. Dependence of (a) the normalized number of hydrogen bonds n_{hb} , (b) the dimensionless heat capacity c , and (c) the distance between the ends of the peptide chain \bar{L} for the molecular complex $(Gly)_{73} \in CNT_{(13,0)}$. Curves 1, 2, and 3 show the dependencies for the 3_{10} -helix chain, and curves 4, 5, and 6 show the dependencies for the α -helix chain. The length of the CNT is $L_{CNT} = 16.14$ nm, the number of atoms is $N_c = 1976$, and at $T = 75$ K, there is a transition from α -helix to 3_{10} -helix.

with the Parameters,

$$q_1 = -0.6397e, \quad q_2 = 0.6159e, \quad q_3 = 0.0238e,$$

$$r_1 = 0.2577\rho/\rho_0, \quad r_2 = 0.9356\rho/\rho_0, \quad r_3 = -1.6237\rho/\rho_0,$$

$$\varepsilon = 0.0079778 \text{ eV}, \quad \sigma = 2.837109 \text{ \AA},$$

where we introduce ρ and ρ_0 as the dynamic and equilibrium lengths of the F–H valence bond and e is the charge of an electron (dimension $[r_i] = \text{\AA}$). Using those parameters, we define the FH molecule with the correct values for the dipole and quadrupole moments,

$$\mu = \sum_{i=1}^3 q_i r_i, \quad Q = \sum_{i=1}^3 q_i (r_i - r_m)^2,$$

where r_m is the distance between the centers of the molecule and the fluorine atom. This approach, the ground-state energy of the dimer $(FH)_2$ agree well with the experimental data of Ref. 75, as well as the results of the quantum calculations.⁷⁶

Consider open armchair and zigzag nanotubes with hydrogen atoms attached to the edge carbon atoms—see Fig. 8. To find the ground state $(FH)_N \in CNT$, it is necessary to solve numerically the problem on the minimum of potential energy of the system (14).

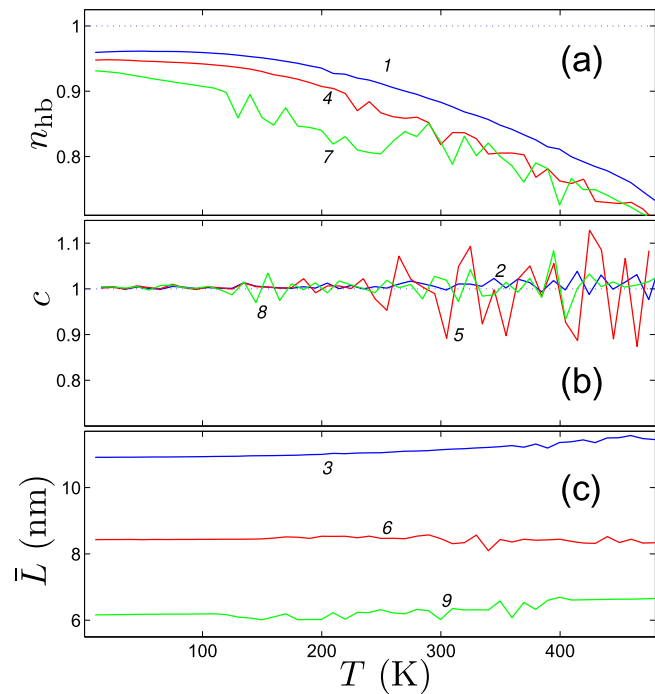


FIG. 6. Dependence of (a) the normalized number of hydrogen bonds n_{hb} , (b) the dimensionless heat capacity c , and (c) the distance between the ends of the peptide chain \bar{L} for the molecular complex $(Gly)_{73} \in CNT$ for nanotube (8,8) (curves 1, 4, 7), (9,9) (curves 2, 5, 8), and (10,10) (curves 3, 6, 9). In nanotube (8,8), the peptide chain is α -helix, in (9,9) is π -helix, and in (10,10) that is β -helix.

By choosing the initial position of the molecules, we can obtain all possible stationary states of the two-component system. At the position of the chain $(FH)_N$ along the outer surface of the nanotube, we obtain a flat zigzag chain of hydrogen bonds with pitch $a = |FF| = 2.49 \text{ \AA}$ and zigzag angle $\alpha = \angle FFF = 117^\circ$. Torsion angle of the chain (dihedral angle formed by four consecutive fluorine atoms) $\phi = \angle FFFF = 180^\circ$.

The numerical solution of the minimum energy problem (14) showed that the hydrogen bond chain (18) retains a flat zigzag shape when placed inside the nanotubes of diameter $D < 0.85$ nm—see Fig. 8 and Table III. The chain pitch a is weakly dependent on the nanotube diameter, the chain zigzag angle α decreases monotonically with increasing diameter, the chain torsion angle $\phi = 180^\circ$ at $D < 0.85$ nm. In the nanotube (11,0) ($D = 0.86$ nm), the chain takes the form of a three-dimensional helix (torsion angle $\phi < 180^\circ$) running along the nanotube surface.

The modeling shows that the hydrogen bond chain closest in The structure to the hydrogen bond chain of the hydroxyl groups (1) is formed by hydrogen fluoride molecules inside nanotubes with chirality indices (6,6) and (10,0). We will, therefore, consider these complexes further.

To avoid the possibility of hydrogen fluoride molecules escaping from the nanotubes, it is better to narrow their open edges as shown in Fig. 9. The small diameter of the edge openings ($D = 0.47$

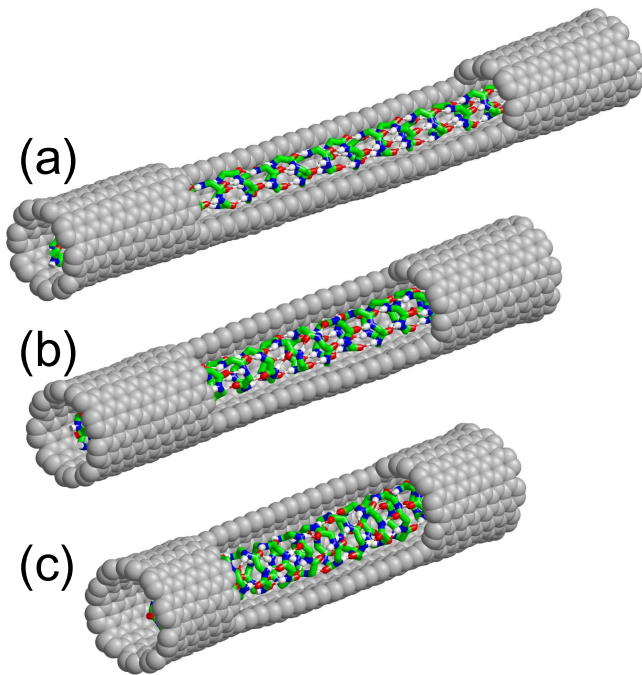


FIG. 7. Configuration of peptide chain $(\text{Gly})_{73}$ in (a) carbon nanotube (8,8) ($L_{\text{cnt}} = 11$ nm), (b) nanotube (9,9) ($L_{\text{cnt}} = 8.8$), and (c) nanotube (10,10) ($L_{\text{cnt}} = 7.3$). The temperature is $T = 300$ K. In nanotube (8,8), the chain is in the form of a α -helix, in nanotube (9,9), that is in the form of a π -helix, and in (10,10), that is in the form of a β -helix. For convenience, some carbon atoms of the nanotubes are not shown.

and 0.42 nm) will prevent a large fluorine atom from leaving but will preserve the possibility of protons leaving and entering. So we get a chain of hydrogen bonds encapsulated in a carbon nanotube: $(\text{FH})_N @ \text{CNT}$. Note that in 2016, endohedral fullerene $\text{HF} @ \text{C}_{60}$ was synthesized containing Buckminsterfullerene inside a molecule of hydrogen fluoride.⁷⁷

Proton transport along the zigzag chain of hydrogen bonds proceeds by migration of two types of defects: ionic and orientational.^{10,20} In the first stage of transport, the proton moves as an ionic defect. There is a sequential movement of hydrogen atoms along the hydrogen bond lines from one fluorine atom to the neighboring one, transferring the chain from the $\dots \text{FH} \cdot \cdot \cdot \text{FH} \cdot \cdot \cdot \text{FH} \cdot \cdot \cdot \text{FH} \cdot \cdot \cdot$ to the $\dots \text{HF} \cdot \cdot \cdot \text{HF} \cdot \cdot \cdot \text{HF} \cdot \cdot \cdot \text{HF} \cdot \cdot \cdot$. In the second stage, an orientation defect (sequential rotation of the FH chain molecules by the zigzag angle α) must pass through the chain to bring the chain back to its original orientation.

Note that the used force field (19) and (20) allows us to model the formation and motion of orientational defects.

The chain of hydrogen bonds inside the nanotube is bistable, and all molecules of the chain can be orientated either from left to right or from right to left. An orientation defect occurs when the molecules of the chain are directed in different directions in the first and second parts of the chain. When the molecules face each other, an excess density of protons appears in the defect localization region,

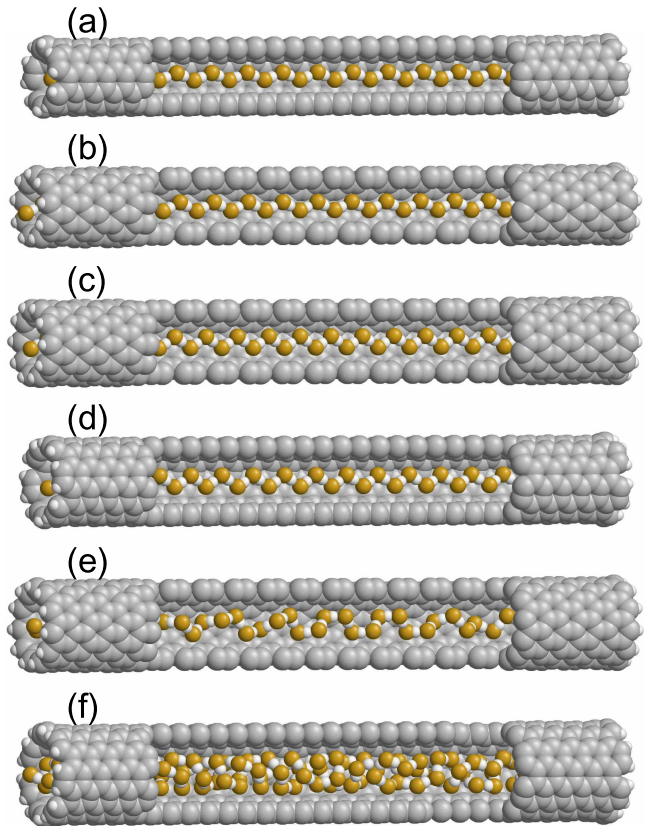


FIG. 8. Stationary state of the hydrogen bond chain $(\text{FH})_N$ inside an open single-walled CNT with chirality index (n, m) : (a) $(\text{FH})_{32} @ \text{CNT}_{(5,5)}$ (nanotube chemical formula $\text{C}_{600}\text{H}_{20}$); (b) $(\text{FH})_{35} @ \text{CNT}_{(9,0)}$ ($\text{C}_{648}\text{H}_{18}$); (c) $(\text{FH})_{38} @ \text{CNT}_{(10,0)}$ ($\text{C}_{720}\text{H}_{20}$); (d) $(\text{FH})_{36} @ \text{CNT}_{(6,6)}$ ($\text{C}_{720}\text{H}_{24}$); (e) $(\text{FH})_{44} @ \text{CNT}_{(11,0)}$ ($\text{C}_{792}\text{H}_{22}$); and (f) $(\text{FH})_{106} @ \text{CNT}_{(7,7)}$ ($\text{C}_{840}\text{H}_{28}$). For ease of review, some atoms of the nanotubes are not shown.

so such a defect is called a positive defect—see Figs. 9(b) and 9(e). When the molecules are directed away from each other in the defect localization region, the proton density decreases, so such a defect is called negative—see Figs. 9(c) and 9(f).

TABLE III. Values of nanotube diameter D , pitch a , and angle α of zigzag and angle of torsion ϕ of hydrogen bonding chain $(\text{FH})_\infty$ inside $\text{CNT}_{(n,m)}$.

(n, m)	D (Å)	a (Å)	α (°)	ϕ (°)
(5,5)	6.8	2.48	138	180
(9,0)	7.1	2.48	132	180
(10,0)	7.8	2.47	114	180
(6,6)	8.1	2.47	113	180
(11,0)	8.6	2.47	108	120
(7,7)	9.5	2.60	88	93

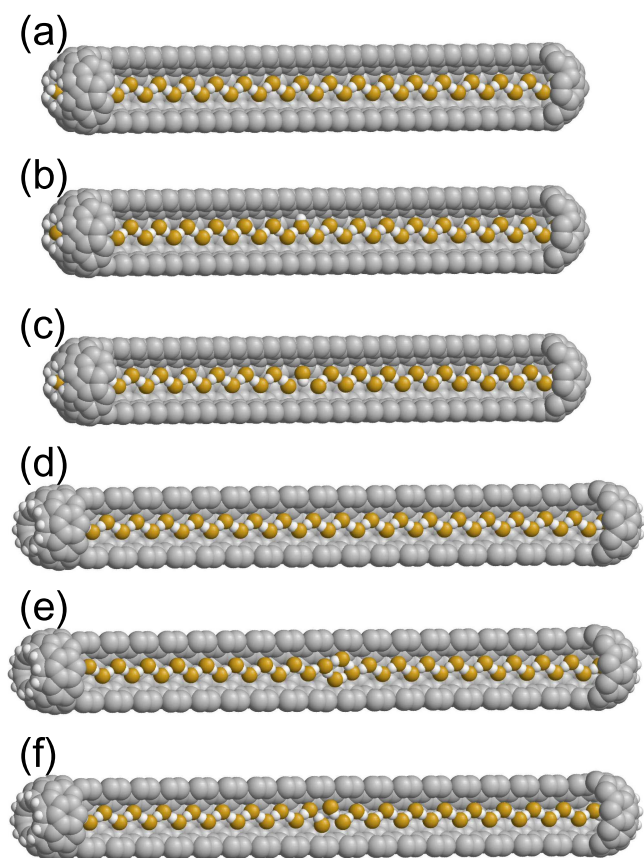


FIG. 9. Stationary state of the hydrogen bond chain $(\text{FH})_N$ inside $\text{CNT}_{(n,m)}$ with narrowed open edges: (a) $(\text{FH})_{36}@\text{CNT}_{(10,0)}$ (nanotube chemical formula $\text{C}_{430}\text{H}_{12}$), ground state; (b) a chain with a positive orientational defect; (c) a chain with a negative orientational defect; (d) $(\text{FH})_{38}@\text{CNT}_{(6,6)}$ ($\text{C}_{402}\text{H}_{20}$), ground state; (e) a chain with a positive orientational defect; (f) a chain with a negative orientational defect (defects are located in the center of the chain). For simplicity, some atoms of the nanotubes are not shown.

The stationary orientational defects of the hydrogen bonding chain $(\text{FH})_N$ inside $\text{CNT}_{(6,6)}$ and $(10,0)$ are shown in Figs. 9(b), 9(c), 9(e), and 9(f). As can be seen from the figure, the orientational defects are localized at three to four chain links. In nanotube $(6,6)$, the energy of positive defect (the difference in the energy of the chain with defect from the energy of the ground state of the chain) is $\Delta E_+ = 0.56$ eV, and the energy of negative defect is $\Delta E_- = 0.51$ eV. In the $(10,0)$ nanotube, the orientational defect energies of the chain $\Delta E_+ = 0.06$ eV, $\Delta E_- = 0.91$ eV.

To test the stability of a chain of hydrogen bonds $(\text{FH})_N$ placed inside a CNT, a molecular dynamics simulation was carried out on a chain of $N = 177$ FH molecules placed inside a $\text{CNT}_{(6,6)}$ with narrowed open edges. With a length of $L = 38.7$ nm, such a nanotube is presented by the formula $\text{C}_{3620}\text{H}_{20}$. A zigzag chain of hydrogen bonds $(\text{FH})_{177}$ completely fills the internal cavity of the nanotube. Such a nanotube of length $L = 8.7$ nm is shown in Fig. 9(d).

Numerical modeling of the system of equations of motion (15) and (16) showed that the chain of hydrogen bonds inside the nanotube, complex $(\text{FH})_{177}@\text{CNT}_{(6,6)}$, at all considered temperatures $T < 500$ K remains stable—it always remains inside and maintains a zigzag shape. At $T < 400$ K, the chain of hydrogen bonds always remains in the initial ground state, and at $T > 400$ K, a positive orientational defect⁷⁸ can already appear at the right end of the chain and then move along it.

Simulation of the dynamics of a complex with an orientational defect in the internal chain of hydrogen bonds showed that the movement of the defects is thermally activated (at low temperatures the defects remain pinned) and occurs in the form of Brownian motion of the particle along the chain. The higher the temperature, the higher the mobility of defects. A positive orientation defect has higher mobility than a negative defect. A defect disappears when it reaches the end of the chain and the chain goes into a homogeneous ground state.

Thus, thermal vibrations do not lead to breaks in the chain of hydrogen bonds $(\text{FH})_\infty$ inside the carbon nanotube, so the chain can always be used for proton transport. When a proton is transferred along a chain of hydrogen bonds, the longest time is required for its reorientation after passing through the ionic defect. This reorientation, the transition of the chain from the $\text{HF}\cdots\text{HF}\cdots\text{HF}\cdots$ state to the $\text{FH}\cdots\text{FH}\cdots\text{FH}\cdots$ state, occurs due to thermally activated passage along the chain of positive orientation defect. Therefore, thermal vibrations not only do not interfere with the transport of protons along the chain of hydrogen bonds inside the nanotube, but they are its necessary condition.

VI. CONCLUSION

Being motivated by the pioneering papers of David Campbell on nonlinear dynamics of molecular structures, here we have studied numerically the structure and dynamics of several types of hydrogen-bonded molecular chains placed inside capped or open-edge carbon nanotubes. We have demonstrated that a polypeptide chain can be stabilized by a carbon nanotube, and it may transform into a helical structure with parallel chains of hydrogen-bonded peptide groups. A chain of hydrogen fluoride molecules placed inside a carbon nanotube of a small radius can create a hydrogen-bonded zigzag chain being highly suitable to support an efficient proton transport. In such molecular systems, the hydrogen-bonded chains retain their structure, being stabilized by the interaction with carbon nanotubes. Our studies have uncovered that for some types of molecular structures, the hydrogen-bonded chains will remain stable up to $T = 500$ K. Thus, the results of our numerical modeling suggest that the use of carbon nanotubes with encapsulated hydrogen fluoride molecules would allow to engineer anhydrous molecular systems supporting high proton conductivity being able to operate at high temperatures.

ACKNOWLEDGMENTS

This work was supported by the Australian Research Council (Grants Nos. DP200101168 and DP210101292). Computational facilities were provided by the Interdepartmental Supercomputer Center of the Russian Academy of Sciences.

AUTHOR DECLARATIONS

Conflict of Interest

The authors have no conflicts to disclose.

Author Contributions

Alexander V. Savin: Conceptualization (equal); Formal analysis (lead); Investigation (lead); Software (lead); Supervision (equal); Writing – original draft (lead); Writing – review & editing (equal).
Yuri S. Kivshar: Conceptualization (equal); Formal analysis (lead); Investigation (lead); Software (lead); Supervision (equal); Writing – original draft (lead); Writing – review & editing (equal).

REFERENCES

- D. K. Campbell, S. Flach, and Y. S. Kivshar, “Localizing energy through nonlinearity and discreteness,” *Phys. Today* **57**, 43 (2004).
- Y. S. Kivshar and D. K. Campbell, “Peierls-Nabarro potential barrier for highly localized nonlinear modes,” *Phys. Rev. E* **48**, 3077 (1993).
- K. Fesser, A. R. Bishop, and D. K. Campbell, “Optical absorption from polarons in a model of polyacetylene,” *Phys. Rev. B* **27**, 4804 (1983).
- L. Pauling, R. B. Corey, and H. R. Branson, “The structure of proteins; two hydrogen-bonded helical configurations of the polypeptide chain,” *Proc. Natl. Acad. Sci. U.S.A.* **37**(4), 205–211 (1951).
- L. Pauling and R. B. Corey, “Atomic coordinates and structure factors for two helical configurations of polypeptide chains,” *Proc. Natl. Acad. Sci. U.S.A.* **37**(5), 235–240 (1951).
- G. Careri, U. Buontempo, F. Galluzzi, A. C. Scott, E. Gratton, and E. Shyamsunder, “Spectroscopic evidence for Davydov-like solitons in acetanilide,” *Phys. Rev. B* **30**(8), 4689–4702 (1984).
- J. C. Eilbeck, P. S. Lomdahl, and A. C. Scott, “Soliton structure in crystalline acetanilide,” *Phys. Rev. B* **30**(8), 4703–4712 (1984).
- S. C. Chowdhury and J. W. Gillespie, Jr., “A molecular dynamics study of the effects of hydrogen bonds on mechanical properties of Kevlar crystal,” *Comput. Mater. Sci.* **148**, 286–300 (2018).
- J. F. Nagle and H. J. Morowitz, “Molecular mechanisms for proton transport in membranes,” *Proc. Natl. Acad. Sci. U.S.A.* **75**(1), 298–302 (1978).
- J. F. Nagle and S. Tristram-Nagle, “Hydrogen bonded chain mechanisms for proton conduction and proton pumping,” *J. Membrane Biol.* **74**, 1–14 (1983).
- K.-D. Kreuer, “Proton conductivity: Materials and applications,” *Chem. Mater.* **8**(3), 610–641 (1996).
- C. Nagamani, U. Viswanathan, C. Versek, M. T. Tuominen, S. M. Auerbach, and S. Thayumanavan, “Importance of dynamic hydrogen bonds and reorientation barriers in proton transport,” *Chem. Commun.* **47**, 6638–6640 (2011).
- R. W. Jansen, R. Bertocini, D. A. Pinnick, A. I. Katz, R. C. Hanson, O. F. Sonkey, and M. O’Keeffe, “Theoretical aspects of solid hydrogen halides under pressure,” *Phys. Rev. B* **35**(18), 9830–9840 (1987).
- M. Sprinborg, “Energy surfaces and electronic properties of hydrogen fluoride,” *Phys. Rev. B* **38**(2), 1483–1503 (1988).
- G. Zundel, “Hydrogen bonds with large proton polarizability and proton transfer processes in electrochemistry and biology,” *Adv. Chem. Phys.* **111**, 1 (2000).
- H. Merz and G. Zundel, “Proton conduction in bacteriorhodopsin VIA a hydrogen-bonded chain with large proton polarizability,” *Biochem. Biophys. Res. Commun.* **101**(2), 540–546 (1981).
- F. Fillaux, “The impact of vibrational spectroscopy with neutrons on our view of quantum dynamics in hydrogen bonds and proton transfer,” *J. Mol. Struct.* **615**, 45–59 (2002).
- D. Marx, “Proton transfer 200 years after von Grothuss: Insights from ab initio simulations,” *Chem. Phys. Chem.* **7**(9), 1848–1870 (2006).
- N. Bjerrum, “Structure and properties of ice,” *Science* **115**(2989), 385–390 (1952).
- L. Onsager, “The motion of ions: Principles and concepts,” *Science* **166**(3911), 1359 (1969).
- V. Y. Antonchenko, A. S. Davydov, and A. V. Zolotaryuk, “Solitons and proton motion in ice-like structures,” *Phys. Status Solidi B* **115**, 631 (1983).
- S. Pnevmatikos, A. V. Savin, A. V. Zolotaryuk, Y. S. Kivshar, and M. J. Velgakis, “Nonlinear transport in hydrogen-bonded chains: Free solitonic excitations,” *Phys. Rev. A* **43**(10), 5518–5536 (1991).
- V. M. Karpan, Y. Zolotaryuk, P. L. Christiansen, and A. V. Zolotaryuk, “Discrete kink dynamics in hydrogen-bonded chains: The two-component model,” *Phys. Rev. E* **70**, 056602 (2004).
- X.-F. Pang, J.-F. Yu, and H.-J. Zeng, “The properties of proton conductivity along the hydrogen-bonded molecular systems with damping under influences of thermal perturbation and structure nonuniformity,” *Int. J. Modern Phys. B* **25**(01), 55–71 (2011).
- M. B. T. Ndjike, A. S. T. Nguetcho, J. Li, and J. M. Bilbault, “Interplay role between dipole interactions and hydrogen bonding on proton transfer dynamics,” *Nonlinear Dyn.* **105**, 2619–2643 (2021).
- A. S. Davydov, “The theory of the absorption of light in molecular crystals,” *Tr. In-ta Fiz. AN UkrSSR*, No. 1, 3–173 (1951).
- W. Moffitt, “Optical rotatory dispersion of helical polymers,” *J. Chem. Phys.* **25**(6), 467–478 (1956).
- A. S. Davydov, *Theory of Molecular Excitons* (Izd. Nauka, Moscow, 1968); A. S. Davydov, *Theory of Molecular Excitons* (Plenum Press, New York, 1971).
- A. S. Davydov, “Deformation of molecular crystals at electronic excitation,” *Phys. Status Solidi* **36**, 211–219 (1969).
- A. S. Davydov and N. I. Kislukha, “Solitary excitations in one-dimensional molecular chains,” *Phys. Status Solidi B* **59**, 465–470 (1973).
- A. S. Davydov and N. I. Kislukha, “Solitons in one-dimensional molecular chains,” *Phys. Status Solidi B* **75**, 735–742 (1976).
- A. S. Davydov, “Solitons in molecular systems,” *Phys. Scr.* **20**, 387–394 (1979).
- A. S. Davydov, “The role of solitons in the energy and electron transfer in one-dimensional molecular systems,” *Physica D* **3**, 1–22 (1981).
- J. M. Hyman, D. W. Mc Laughlin, and A. C. Scott, “On Davydov’s alpha-helical solitons,” *Physica D* **3**, 23–45 (1981).
- A. C. Scott, “Dynamics of Davydov solitons,” *Phys. Rev. A* **26**, 578–595 (1982).
- P. S. Lomdahl, S. P. Layne, and I. J. Bigio, “Solitons in biology,” *Los Alamos Sci.* **10**, 2–22 (1984), see <https://library.lanl.gov/cgi-bin/getfile?10-01.pdf>.
- A. C. Scott, “Davydov solitons in polypeptides,” *Philos. Trans. R. Soc., London A* **315**, 423–436 (1985).
- A. C. Scott, “Davydov’s soliton,” *Phys. Rep.* **217**, 1–67 (1992).
- P. S. Lomdahl and W. C. Kerr, “Do Davydov solitons exist at 300 K?,” *Phys. Rev. Lett.* **55**(11), 1235–8 (1985).
- V. A. Kuprievich, “On autolocalization of the stationary states in a finite molecular chain,” *Physica D* **14**(3), 395–402 (1985).
- L. S. Brizhik, Y. B. Gaididei, A. A. Vakhnenko, and V. A. Vakhnenko, “Soliton generation in semi-infinite molecular chains,” *Phys. Status Solidi B* **146**(2), 605–12 (1988).
- A. V. Savin and A. V. Zolotaryuk, “Dynamics of the amide-I excitation in a molecular chain with thermalized acoustic and optical modes,” *Physica D* **68**(1), 59–64 (1993).
- L. S. Brizhik, “Soliton generation in molecular chains,” *Phys. Rev. B* **48**(5), 3142–3144 (1993).
- A. V. Zolotaryuk, K. H. Spatschek, and A. V. Savin, “Bifurcation scenario of the Davydov-Scott self-trapping mode,” *Europhys. Lett.* **31**(9), 531–536 (1995).
- L. Brizhik, A. Eremko, B. Piette, and W. Zakrzewski, “Solitons in α -helical proteins,” *Phys. Rev. E* **70**, 031914 (2004).
- D. D. Georgiev and J. F. Glazebrook, “Launching of Davydov solitons in protein α -helix spines,” *Phys. E* **124**, 114332 (2020).
- D. D. Georgiev and J. F. Glazebrook, “Thermal stability of solitons in protein α -helices,” *Chaos, Solitons Fract.* **155**, 111644 (2022).
- L. Cruzeiro, “The VES hypothesis and protein conformational changes,” *Z. Phys. Chem.* **230**(5–7), 743–776 (2016).
- L. Cruzeiro, “The VES KM: A pathway for protein folding in vivo,” *Pure Appl. Chem.* **92**(1), 179–191 (2020).

- ⁵⁰L. Cruzeiro, “Knowns and unknowns in the Davydov model for energy transfer in proteins,” *Fiz. Nizk. Temp.* **48**, 1105–1126 (2022).
- ⁵¹A. S. Davydov, “Influence of electron-phonon interaction on the motion of an electron in a one-dimensional molecular system,” *Theor. Math. Phys.* **40**(3), 831–840 (1979).
- ⁵²A. S. Davydov and A. V. Zolotareyuk, “Subsonic and supersonic solitons in nonlinear molecular chains,” *Phys. Scripta* **30**, 426–430 (1984).
- ⁵³A. S. Davydov, *Solitons in Molecular Systems* (Reidel, Dord-recht, 1991).
- ⁵⁴W. D. Cornell, W. P. Cieplak, C. I. Bayly, I. R. Gould, K. M. Merz, D. M. Ferguson, D. C. Spellmeyer, T. Fox, J. W. Caldwell, and P. A. Kollman, “A second generation force field for the simulation of proteins, nucleic acids, and organic molecules,” *J. Am. Chem. Soc.* **117**, 5179–5197 (1995).
- ⁵⁵W. C. Swope, H. C. Andersen, P. H. Berens, and K. R. Wilson, “A computer simulation method for the calculation of equilibrium constants for the formation of physical clusters of molecules: Application to small water clusters,” *J. Chem. Phys.* **76**, 637 (1982).
- ⁵⁶G. R. Liu, Y. Cheng, D. Mi, and Z. R. Li, “A study on self-insertion of peptides into single-walled carbon nanotubes based on molecular dynamics simulation,” *Int. J. Modern Phys.* **16**(08), 1239–1250 (2005).
- ⁵⁷P. Xiu, Z. Xia, and R. Zhou, “Small molecules and peptides inside carbon nanotubes: Impact of nanoscale confinement,” in *Physical and Chemical Properties of Carbon Nanotubes*, edited by Satoru Suzuki (IntechOpen, 2013).
- ⁵⁸Z.-S. Zhang, Y. Kang, L.-J. Liang, Y.-C. Liu, T. Wu, and Q. Wang, “Peptide encapsulation regulated by the geometry of carbon nanotubes,” *Biomaterials* **35**(5), 1771–1778 (2014).
- ⁵⁹A. V. Savin, Y. S. Kivshar, and B. Hu, “Suppression of thermal conductivity in graphene nanoribbons with rough edges,” *Phys. Rev. B* **82**, 195422 (2010).
- ⁶⁰A. V. Savin and Y. S. Kivshar, “Phononic Fano resonances in graphene nanoribbons with local defects,” *Sci. Rep.* **7**, 4668 (2017).
- ⁶¹A. V. Savin and Y. S. Kivshar, “Discrete breathers in carbon nanotubes,” *Europhys. Lett.* **82**, 66002 (2008).
- ⁶²G. Hummer, J. Rasaiah, and J. Noworyta, “Water conduction through the hydrophobic channel of a carbon nanotube,” *Nature* **414**, 188 (2001).
- ⁶³C. Dellago, M. M. Naor, and G. Hummer, “Proton transport through water-filled carbon nanotubes,” *Phys. Rev. Lett.* **90**(10), 105902 (2003).
- ⁶⁴J. Kofinger, G. Hummer, and C. Dellago, “Single-file water in nanopores,” *Phys. Chem. Chem. Phys.* **13**(34), 15403–15417 (2011).
- ⁶⁵B. H. S. Mendonca, D. N. de Freitas, M. H. Kohler, R. J. C. Batista, M. C. Barbosa, and A. B. de Oliveira, “Diffusion behaviour of water confined in deformed carbon nanotubes,” *Physica A* **517**, 491–498 (2019).
- ⁶⁶M. Druchok, V. Krasnov, T. Krokhmalkii, T. C. E. Bufalo, S. M. de Souza, O. Rojas, and O. Derzhko, “Toward a quasiphase transition in the single-file chain of water molecules: Simple lattice model,” *J. Chem. Phys.* **158**(10), 104304 (2023).
- ⁶⁷J. Chen, X.-Z. Li, Q. Zhang, A. Michaelides, and E. Wang, “Nature of proton transport in a water-filled carbon nanotube and in liquid water,” *Phys. Chem. Chem. Phys.* **15**, 6344–6349 (2013).
- ⁶⁸X. Ma, C. Li, A. B. F. Martinson, and G. A. Voth, “Water-assisted proton transport in confined nanochannels,” *Phys. Chem. C* **124**(29), 16186–16201 (2020).
- ⁶⁹I. Hanasaki, A. Nakamura, T. Yonebayashi, and S. Kawano, “Structure and stability of water chain in a carbon nanotube,” *J. Phys.: Condens. Matter* **20**, 015213 (2008).
- ⁷⁰M. Atoji and W. N. Lipscomb, “The crystal structure of hydrogen fluoride,” *Acta Crystallogr.* **7**, 173 (1954).
- ⁷¹E. A. Orabi and J. D. Faraldo-Gomez, “A new molecular-mechanics model for simulations of hydrogen fluoride in chemistry and biology,” *J. Chem. Theory Comput.* **16**(8), 5105–5126 (2020).
- ⁷²A. Roztoczynska, J. Koztowska, P. Lipkowski, and W. Bartkowiak, “Hydrogen bonding inside and outside carbon nanotubes: HF dimer as a case study,” *Phys. Chem. Chem. Phys.* **18**, 2417 (2016).
- ⁷³W. F. Gtari and B. Tangour, “Interaction of HF, HBr, HCl and HI molecules with carbon nanotubes,” *Acta Chim. Slov.* **65**, 289 (2018).
- ⁷⁴M. E. Cournoyer and W. L. Jorgensen, “An improved intermolecular potential function for simulations of liquid hydrogen fluoride,” *Mol. Phys.* **51**, 119 (1984).
- ⁷⁵T. R. Dyke, B. J. Howard, and W. Klemperer, “Radiofrequency and microwave spectrum of the hydrogen fluoride dimer; a nonrigid molecule,” *J. Chem. Phys.* **56**, 2442 (1972).
- ⁷⁶A. V. Nemukhin, *Zh. Fiz. Khim.* **66**, 4 (1992).
- ⁷⁷A. Krachmalnicoff, R. Bounds, S. Mamone, S. Alom, M. Concistre, B. Meier, K. Kouril, M. E. Light, M. R. Johnson, S. Rols, A. J. Horsewill, A. Shugai, U. Nagel, T. Room, M. Carravetta, M. H. Levitt, and R. J. Whitby, “The dipolar endofullerene HF@C60,” *Nat. Chem.* **8**, 953–957 (2016).
- ⁷⁸A. V. Savin and O. I. Savina, “The structure and dynamics of the chains of hydrogen bonds of hydrogen fluoride molecules inside carbon nanotubes,” *Phys. Solid State* **62**(11), 2217–2223 (2020).